Application of the Finite Element Method to Inverse Problems in Solid Mechanics

Brian H. Dennis[1], Weiya Jin[2], George S. Dulikravich[3], Jovo Jaric[4]

[1]Department of Mechanical and Aerospace Engineering, University of Texas at Arlington,Arlington, TX, U.S.A.
[2]College of Mechanical Engineering, Zhejiang University of Technology, ZJUT, Hangzhou, Zhejiang, China
[3]Department of Mechanical and Materials Engineering, Florida International University, Miami, FL, U.S.A.
[4]Faculty of Mathematics, University of Belgrade, Belgrade, Serbia.

Abstract

This paper presents the application of the finite element method to two inverse problems in solid mechanics. In the first application, a formulation for the inverse detection of unknown boundary conditions for thermoelastic problems is detailed. The second application involves the inverse determination of heterogeneous material properties for a loaded structure. Both approaches involve the use of finite element models and over-specified boundary information such as displacements, reaction forces, and reaction moments to inversely determine unknown quantities.

1. Introduction

The finite element method has recently been extended beyond simple analysis and has been applied to various shape and material optimization applications. However, its utility in the solution to inverse problems is relatively less known. In this paper we present the application of the finite element method to two different inverse problems involving structural objects. In the first application, a finite element formulation for the inverse detection of unknown boundary conditions for thermoelastic problems is presented. The second application involves the use of the finite element method for inversely determine spatially varying material properties of a structure using measurements of displacements, reaction forces, and reaction moments.

2. Inverse Detection of Unknown Boundary Conditions.

It is sometimes difficult or impossible to place temperature probes, heat flux probes, or strain gauges on certain parts of a surface of a solid body because of its small size, geometric inaccessibility, or exposure to a hostile environment. With an appropriate inverse method, these unknown boundary values can be determined from additional information provided at the boundaries where such values can be measured. That is, for inverse problems, the unknown boundary conditions on parts of the boundary can be determined by over-specifying the boundary conditions (enforcing both Dirichlet and Neumann type boundary conditions simultaneously) on at least some of the remaining portions of the boundary, and providing either Dirichlet or Neumann type boundary conditions on the rest of the boundary. It is possible, after a series of algebraic manipulations, to transform the original system of equations into a system which enforces the over-specified boundary conditions and includes the unknown boundary conditions as a part of the unknown solution vector.

In the case of steady thermal and elastic problems, the objective of the inverse problem is to determine displacements, surface stresses, heat fluxes, and temperatures on boundaries where they are unknown. The problem of inverse determination of unknown boundary conditions in two-dimensional steady heat conduction has been solved by a variety of methods (Larsen, 1985; Hensel and Hills, 1989; Martin and Dulikravich, 1996; Dennis and Dulikravich, 1999; Dennis et al. 2004; Olsen and Throne, 2000). Similarly, a separate inverse boundary condition determination problem in linear elastostatics has been solved by different methods (Martin et al. 1995). The inverse boundary condition determination problem for steady thermoelasticity was also solved for several two-dimensional and three-dimensional problems (Dennis and Dulikravich, 1999; Dennis et al. 2004).

---

[1]Corresponding author - Email: *dennisb@uta.edu*

A 3-D finite element formulation is presented here that allows one to solve this inverse problem in a direct manner by over-specifying boundary conditions on boundaries where such additional information is available. Our objective is to develop and demonstrate an approach for the prediction of thermal and elasticity boundary conditions on parts of a three-dimensional solid body surface by using a finite element approach (FEA).

2.1 Three-dimensional Formulation for Thermoelasticity

The Navier equations for linear static deformations u, v, w in three-dimensional Cartesian x, y, z coordinates are

$$(\lambda + G)\left(\frac{\partial^2 u}{\partial x^2} + \frac{\partial^2 v}{\partial x \partial y} + \frac{\partial^2 w}{\partial x \partial z}\right) + G\nabla^2 u + X = 0 \tag{1}$$

$$(\lambda + G)\left(\frac{\partial^2 u}{\partial x \partial y} + \frac{\partial^2 v}{\partial y^2} + \frac{\partial^2 w}{\partial y \partial z}\right) + G\nabla^2 v + Y = 0 \tag{2}$$

$$(\lambda + G)\left(\frac{\partial^2 u}{\partial x \partial z} + \frac{\partial^2 v}{\partial y \partial z} + \frac{\partial^2 w}{\partial z^2}\right) + G\nabla^2 w + Z = 0 \tag{3}$$

Where,

$$\lambda = \frac{E\nu}{(1+\nu)(1-2\nu)}, \qquad G = \frac{E}{2(1+\nu)}$$

Here, X, Y, Z are body forces per unit volume due to stresses from thermal expansion, ν is the Poisson's ratio, G is the shear modulus, E is the Young's modulus of elasticity, and λ is Lame's constant.

$$X = -(3\lambda + 2G)\frac{\partial \alpha \Delta \theta}{\partial x} \tag{4}$$

$$Y = -(3\lambda + 2G)\frac{\partial \alpha \Delta \theta}{\partial y} \tag{5}$$

$$Z = -(3\lambda + 2G)\frac{\partial \alpha \Delta \theta}{\partial z} \tag{6}$$

Here, α is the coefficient of thermal expansion and θ is the temperature. This system of partial differential equations was discretized using the typical Galerkin finite element approach (Huebner et al. 1995; Hughes, 2000) on eight-node hexahedral elements. The approach leads to a symmetric local stiffness matrix, $[K^e]$, and a force per unit volume vector, $\{f^e\}$, which are determined for each finite element in the domain and then assembled into the global system of algebraic equations

$$[K]\{\delta\} = \{F\} \tag{7}$$

After applying boundary conditions, the global displacements, $\{\delta\}$, are found by solving this system of linear algebraic equations. The stresses, $\{\sigma\}$, can then be found by differentiating the displacements.

2.2 Three-dimensional Formulation for the Thermal Problem

The temperature distribution throughout the isotropic solid three-dimensional domain can be found by solving Poisson's equation for steady linear heat conduction with a distributed steady heat source function, Q, and thermal conductivity coefficient, k.

$$-k\left(\frac{\partial^2 \theta}{\partial x^2} + \frac{\partial^2 \theta}{\partial y^2} + \frac{\partial^2 \theta}{\partial z^2}\right) = Q \tag{8}$$

Applying the Galerkin finite element method over an element results in the local stiffness matrix, $[K_c^e]$, and heat flux vector, $\{Q^e\}$, which are determined for each finite element in the domain and then assembled into the global system of algebraic equations

$$[K_c]\{\theta\} = \{Q\} \tag{9}$$

2.3 Direct and Inverse Formulations

Thus, the equations for steady thermoelasticity were discretized by using a Galerkin finite element method. This resulted in two linear systems of algebraic equations

$$[K]\{\delta\}=\{F\}, \qquad [K_c]\{\theta\}=\{Q\} \tag{10}$$

The systems are typically large, sparse, symmetric, and positive definite. Once the global system has been formed, the boundary conditions are applied. For a well-posed analysis (direct) problem, the boundary conditions must be known on all boundaries of the domain. For heat conduction, either the temperature, θ_s, or the heat flux, Q_s, must be specified at each point of the boundary. For elasticity, either stress or deformation must be specified on each boundary.

For an inverse problem, the unknown boundary conditions on parts of the boundary can be determined by enforcing over-specified boundary conditions on at least some of the boundary, and providing either Dirichlet or Neumann type boundary conditions on the rest of the boundary. As an example, consider the linear system for heat conduction on a tetrahedral finite element with boundary conditions given at nodes 1 and 4.

$$\begin{bmatrix} K_{11} & K_{12} & K_{13} & K_{14} \\ K_{21} & K_{22} & K_{23} & K_{24} \\ K_{31} & K_{32} & K_{33} & K_{34} \\ K_{41} & K_{42} & K_{43} & K_{44} \end{bmatrix} \begin{Bmatrix} \theta_1 \\ \theta_2 \\ \theta_3 \\ \theta_4 \end{Bmatrix} = \begin{Bmatrix} Q_1 \\ Q_2 \\ Q_3 \\ Q_4 \end{Bmatrix} \tag{11}$$

As an example of an inverse problem, one could specify both the temperature, θ_s, and the heat flux, Q_s, at node 1, flux only at nodes 2 and 3, and assume the boundary conditions at node 4 as being unknown. The original system of equations (11) can be modified by adding a row and a column corresponding to the additional equation for the over-specified flux at node 1 and the additional unknown due to the unknown boundary flux at node 4. The result is

$$\begin{bmatrix} 1 & 0 & 0 & 0 & 0 \\ K_{21} & K_{22} & K_{23} & K_{24} & 0 \\ K_{31} & K_{32} & K_{33} & K_{34} & 0 \\ K_{41} & K_{42} & K_{43} & K_{44} & -1 \\ K_{11} & K_{12} & K_{13} & K_{14} & 0 \end{bmatrix} \begin{Bmatrix} \theta_1 \\ \theta_2 \\ \theta_3 \\ \theta_4 \\ Q_4 \end{Bmatrix} = \begin{Bmatrix} \theta_s \\ Q_2 \\ Q_3 \\ 0 \\ Q_s \end{Bmatrix} \tag{12}$$

The resulting systems of equations will remain sparse, but will be non-symmetric and possibly rectangular (instead of square) depending on the ratio of the number of known to unknown boundary values.

2.4 Regularization

A regularization method was applied to the solution of the systems of equations in attempts to increase the method's tolerance for measurement errors in the over-specified boundary conditions. Different regularization methods for the 3-D formulation were given previously (Dennis et al. 2004). Here, we consider the regularization of the inverse heat conduction problem.

The general form of a regularized system is given as (Neumaier, 1998):

$$\begin{bmatrix} K_c \\ \Lambda D \end{bmatrix} \{\theta\} = \begin{Bmatrix} Q \\ 0 \end{Bmatrix} \tag{13}$$

The traditional Tikhonov regularization is obtained when the damping matrix, $[D]$, is set equal to the identity matrix. Solving (13) in a least squares sense minimizes the following error function.

$$error(\theta) = \left\| [K_c]\{\theta\} - \{Q\} \right\|_2^2 + \left\| \Lambda[D]\{\theta\} \right\|_2^2 \tag{14}$$

This represents the least squares minimization of the residual plus a penalty term. The form of the damping matrix determines what penalty is used and the damping parameter, Λ, weights the penalty for each equation. These weights should be determined according to the error associated with the respective equation.

In order to minimize the error in the domain of the object, this regularization method uses Laplacian smoothing of the unknown temperatures and displacements only on the boundaries where the boundary conditions are unknown. This method could be considered a "second order" Tikhonov method. A penalty term can be constructed such that curvature of the solution on the boundaries where boundary conditions are unknown is minimized along with the residual.

$$\left\| \nabla^2 \theta_{ub} \right\|_2^2 \rightarrow \min \tag{15}$$
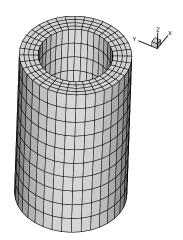
Fig. 1. Surface mesh for test case.

For problems that involve unknown vector fields, such as displacements, Eqn. (15) is modified to smooth a certain component of the field.

$$\left\| \nabla^2 \left(\vec{n} \cdot \{ \delta_{ub} \} \right) \right\|_2^2 \rightarrow \min \tag{16}$$

Here, the normal component of the vector displacement field $\{\delta\}$ is minimized at the unknown boundary. The Laplacian operator in the Eqns. (15) and (16) can be discretized on the object's surface mesh using the method of weighted residuals. This leads to the damping matrix, $[D]$. For heat conduction, this results in the following expression.

$$\left\| [D] \{\theta_{ub}\} \right\|_2^2 = \left\| [K_c] \{\theta_{ub}\} \right\|_2^2 \tag{17}$$

In three-dimensional problems, $[K_c]$ is computed by integrating over surface elements on the boundaries that have unknown boundary conditions. The damping matrix is essentially an assembly of boundary elements that make up the boundary of the object where the boundary conditions are unknown. The local matrix for each element is formed by discretizing the Laplacian operator by the Galerkin weighted residual method. The main advantage of this method is its ability to smooth the solution vector without necessarily driving its components to zero and away from the true solution.

2.5 Solution of the Linear System

In general, the resulting FEM systems for inverse thermoelastic problems are sparse, non-symmetric, and often rectangular (instead of square). These properties make the process of finding an accurate solution to the system quite challenging. One possible approach is to use iterative methods suitable for least squares problems. One such method is the LSQR method, which is an extension of the well known conjugate gradient (CG) method (Paige and Saunders, 1982). The LSQR method and other similar methods such as the conjugate gradient for least squares (CGLS) solve the normalized system, but without explicit computation of $[K]^T[K]$. These methods need only matrix-vector products at each iteration and therefore only require the storage of $[K]$ so they are attractive for solutions of large matrices. However, convergence rates of these methods depend strongly on the condition number of the normalized system that is the condition number of $[K]$ squared (Comino and Gallego, 2005). Therefore, solver performance degrades significantly as the size of the finite element model increases. Convergence can be slow when solving the systems resulting from the inverse finite element discretization since they are naturally ill-conditioned problems.

2.6 Numerical Results

The accuracy and efficiency of the finite element inverse formulation was tested on a simple three-dimensional problem. The method was implemented in an object-oriented finite element code written in C++. Elements used in the calculations were of hexahedral shape with tri-linear interpolation functions. The linear systems were solved with a sparse LSQR method (Paige and Saunders, 1982) with column scaling.
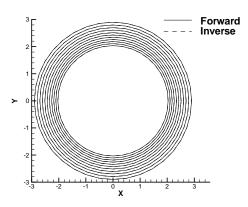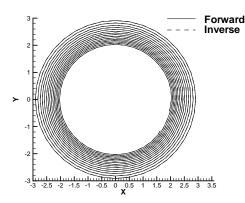
Fig. 2. **C**omputed isotherms on *x - y* plane at *z = 5.0 m* for forward and inverse cases

Fig. 3. Computed displacement magnitude on *x - y* plane at *z = 5.0 m* for

Fig. 4. Computed normal stress (σ_{xx}) on *x - y* plane at *z = 5.0 m* for forward and inverse

Table 1. Values of temperature and pressure used to construct linearly varying boundary conditions on the cylinder surfaces
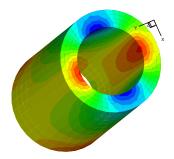
Cylinder	$T_{z-0}(°C)$	$T_{z-10}(°C)$	$P_{z-0}(Pa)$	$P_{z-10}(Pa)$
Interior	6.0	1.0	2.0	1.0
Exterior	10.0	10.0	-	-

The test case involved an annular domain composed of an outer cylinder with length 10.0 m and diameter of 6.0 *m*. The cylindrical hole that passes completely through the cylinder has a diameter of 4.0 *m*. The hexahedral mesh is shown in Figure 1 and is composed of 1440 elements and 1980 nodes. The inner and outer boundaries each have 396 nodes.

This case considers thermal and elastic boundary conditions that vary in all coordinate directions thereby creating a truly three-dimensional example. In the case of a well-posed (analysis) problem, interior boundary conditions were specified as changing linearly along the z-axis. The exact values used at different z-locations are given in Table 1. On the outer cylinder, the displacement was set to zero and a fixed temperature of 10°C was specified. Adiabatic and stress free conditions were specified at the ends of the cylinder. The following material properties were used: $E = 1.0 Pa$, $\nu = 0.0$, $\alpha = 2.0 \times 10^{-2} K^{-1}$, $k = 1.0 W\ m^{-1}K^{-1}$.

The inverse problem was generated by over-specifying the outer cylindrical boundary with the double-precision values of temperatures, normal derivatives of temperature, displacements, and surface tractions obtained from the forward analysis case. At the same time, no boundary conditions were specified on the inner cylindrical boundaries. No errors were used in the over-specified boundary data.

Regularization was used with $\Lambda = 8.5 \times 10^{-5}$. Our experience indicates that a good value for the damping parameter, Λ, is geometry and boundary condition dependent. Currently, the damping parameter is chosen based on experience by first choosing a small value and gradually increasing it until the numerical oscillations in the unknown boundary solution are removed.
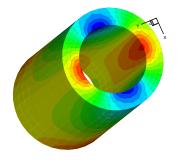
Fig. 5. Computed normal stress (σ_xx) for forward case   Fig. 6. Computed normal stress (σ_xx) for inverse case

The linear system was solved using the LSQR method with column scaling. The LSQR iterations were terminated after the Euclidean norm of the residual of the normal system was less than 1.0×10^{-6}. In this example 2624 LSQR iterations were required for the thermoelastic solution, while 1410 iterations were needed to find the temperature field. The thermoelastic solution consumed about 1.1 minute of computing time on a 3.4GHz Pentium 4 workstation.

The average error between the inverse and direct solutions on the unknown boundaries was 0.02% for temperature and 5.6% for displacement. The direct and inverse temperature contours for a section of the domain are shown in Fig. 2. There is excellent agreement on all sections between the direct and inverse temperature contours. The direct and inverse displacement magnitude contours at the middle section of the domain are shown in Fig. 3 demonstrating that inverse solution is almost identical to the forward solution. Finally, the stress contours for the forward and inverse cases are shown in Fig. 4. The maximum difference between the forward and inverse stresses is less than one percent.

A three-dimensional visualization of the forward and inverse results is shown in Fig. 5 and Fig. 6, respectively. The axial variation of the stress is identical between the inverse and forward calculations.

2.7 Summary for Inverse Determination of Thermo elasticity Boundary Conditions

A formulation for the inverse determination of unknown steady boundary conditions in heat conduction and thermo elasticity for three-dimensional problems has been developed using FEM. The formulation can predict the unknown boundary temperatures and displacements with high accuracy using proper regularization. Reasonable results were obtained by LSQR with column scaling in less than 3,000 iterations for displacements and 1,500 iterations for temperature. Although iterations are required with the LSQR method, it requires much less memory and is more robust than sparse direct solvers for rectangular systems, such as QR factorization. Further research is also needed to improve regularization for inverse problems in elasticity over complicated domains.
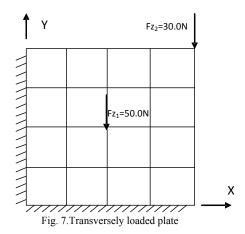
3. Inverse Determination of Material Properties from Boundary Measurements

There are a number of practical problems that involve the inverse determination of material properties using direct measurements taken from a structure. For example, researchers proposed a non-destructive test method for finding flaws in composite laminates using electrical potential measurements (Zhang and Kumar, 2010). The measurements were used together with a numerical model to estimate the bulk conductivity of the panel. Variations in conductivity reveal manufacturing flaws, such as delaminations between the fiber layers. Several authors have proposed inverse methods for determining material parameters using deformations and/or strain measurements (Yuan and Özisik, 1996; Comino and Gallego, 2005; Furukawa et al. 2008). Many of these methods employ numerical models that are based on boundary or finite element methods that are then coupled with optimization algorithms.

If gradient-based optimization methods are considered, the sensitivity of the objective function and constraints with respect to a design parameter is required. If the objective function depends on a finite element calculation, the sensitivity of the response is ultimately required. Methods that can compute these responses accurately and efficiently for inverse problems are therefore needed (Cooreman et al. 2007).

3.1 Inverse Problem Formulation for Determining Modulus of Elasticity Variation

In this section, we consider the inverse determination of heterogenous material properties in a load bearing structure. For simplicity, we will work with a *1.0 m x 1.0 m* plate that is fixed on two ends and under two transverse point loads as shown in Fig. 7. The plate thickness is *0.2 m*. The forward (analysis) problem can be solved with a straightforward application of the finite element method. In our case, this involved discretizing the plate with 16 four-

Fig. 7.Transversely loaded plate

node isoparametric elements of the shear deformable displacement formulation (Mindlin plate elements) (Huebner et al. 1995; Hughes, 2000) as shown in Fig. 7. The modulus of elasticity, *E*, was assumed to be a bilinear function of *x* and *y*. This function was parameterized by using the modulus value at each of the four corners of a finite element as shown in the equation below

$$E(x,y) = (E_2 - E_1)x^2 + (E_4 - E_1)y^2 + (E_1 - E_2 + E_3 - E_4)xy + E_1 \tag{18}$$

In this inverse problem, the objective was to determine the values of *{E}={E₁,E₂,E₃,E₄}* such that the finite element model produces responses that match measured values. These measurements might be displacements, strains, or stresses in the interior or on the boundary of the structure. This inverse problem can then be formulated as a non-linear unconstrained minimization problem of the sum of normalized least squares differences between the computed responses and the measured responses (Eqn. 19).

$$objective = 100.0 * \sqrt{\sum_{i=1}^{m} \left(\frac{R_i - \widetilde{R}_i}{\widetilde{R}_i} \right)^2} \tag{19}$$

Here, *m* is the number of measurements, $\widetilde{R}_i$ is the measured response, and R_i is the computed response. This objective function is essentially the *L2*-norm of the percent error in the computed responses.

Equation 19 can be minimized using a suitable numerical optimization algorithm based on search methods that are local, global, or a combination of both. If a local search is employed, the sensitivities of the objective function (Eqn. 19) to the design variables (values of the Young's modulus of elasticity at each grid point) are typically required. This is a particularly attractive approach if the sensitivities are available directly from the finite element analysis program. In addition, these sensitivities can also be used to guide our choices regarding what measurement data to collect and where it should be collected.

3.2 *Calculating Sensitivities*

Many sophisticated approaches have been proposed for obtaining sensitivities of finite element responses including automatic differentiation (Liu and Der Kiureghian, 1989; Zhang and Der Diureghian, 1993) and the adjoint variable approach (Lee, 1999). However, the simple finite difference approach remains popular due to its programming simplicity and generality since very few modifications to the analysis code are required.

In practice, the semi-analytical method (SAM) is typically used in large scale finite element programs for computing sensitivities. This method combines analytical differentiation with finite differencing to create an approach that is more computationally efficient for large numbers of design parameters. However, the semi-analytical approach, like finite differencing, can lead to inaccurate sensitivities if the perturbation size is not chosen carefully (Barthelemy et al. 1988; Cheng et al. 1989; Barthelemy and Haftka, 1990; Olhoff and Rasmussen, 1991). The optimal perturbation size is not known *a priori*.

An alternative approach is the complex variable semi-analytical method (CVSAM) (Jin et al. 2010a, 2009, 2010b). This method can compute the sensitivities of finite element responses with respect to design variables with high accuracy and efficiency. The method will be introduced briefly in this section.
The finite element global equilibrium equation is
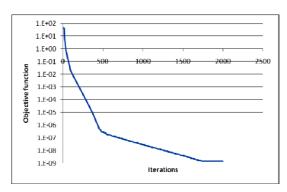
$$[K]\{u\} = \{f\} \tag{20}$$

Fig. 8.Convergence history for Case 1

where $[K]$ is the stiffness matrix, $\{u\}$ is the displacement and $\{f\}$ is the load vector. These are functions of input design variables $\{X\} = \{X_1, X_2, \cdots, X_n\}$.

The SAM combines the efficiency of the analytical method with the ease of use and general nature of the finite difference method. First, we differentiate Equation (20) on both sides and obtain

$$\frac{\partial[K]}{\partial\{X\}}\{u\} + [K]\frac{\partial\{u\}}{\partial\{X\}} = \frac{\partial\{f\}}{\partial\{X\}} \tag{21}$$

Then the derivative of displacement with respect to variables $\{X\}$ can be written as

$$\frac{\partial\{u\}}{\partial\{X\}} \approx \frac{\{\Delta u\}}{\{\Delta X\}} = [K]^{-1}\left(\frac{\{\Delta f\}}{\{\Delta X\}} - \frac{[\Delta K]}{\{\Delta X\}}\{u\}\right) \tag{22}$$

In Equation (21), the same global stiffness matrix $[K]$ is used for computing displacement $\{u\}$ and displacement sensitivity $\partial\{u\}/\partial\{X\}$. The most time consuming computation, $[K]^{-1}$, is calculated only once for Equation (20) and then reused in Equation (22). This advantage makes the SAM programming convenient and computationally efficient. However, since the finite difference method (FDM) is used in Equation (22) to compute $\{\Delta K\}/\{\Delta X\}$ and $\{\Delta f / \Delta X\}$, the SAM inherits the drawback of the FDM. The accuracy of the sensitivity $\partial\{u\}/\partial\{X\}$ computed by the SAM depends on the perturbation size, $\{\Delta X\}$. An optimal perturbation size exists that is small enough to minimize the truncation error but large enough to avoid subtractive cancellation error. The choice of proper perturbation size becomes very difficult for a complex problem when computing sensitivities with respect to multiple variables.

The issue with choice of perturbation size can be eliminated if we consider finite differencing in the complex plane. In this approach, a Taylor series expansion that takes a perturbation in the imaginary dimension is used (Martins, et al. 2003).

$$f(x + i\Delta x) = f(x) + i\Delta x f'(x) - \frac{\Delta x^2 f''(x)}{2!} - \frac{i\Delta x^3 f'''(x)}{3!} + \cdots \tag{23}$$

Grouping the real and imaginary parts of Equation (23), the first order derivative can be obtained as
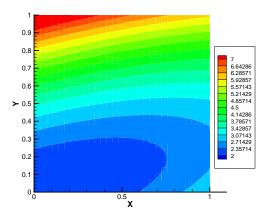
$$f'(X) = \frac{\mathrm{Im}[f(x + i\Delta x)]}{\Delta x} + O(\Delta x^2) \tag{24}$$

We note that the calculation of the first order derivatives in equation (24) does not involve the subtraction of two numbers. Therefore, this approach avoids the subtractive cancellation errors that plague the typical finite difference approach. The perturbation size can be smaller than 10^{-100} without any loss of accuracy.

The CVSAM is obtained when we combine equation (24) with equation (22). The sensitivity of the response to design variable Xi, is given in the following equation.

$$\frac{\partial\{u\}}{\partial X_i} \approx [K]^{-1}\left\{\frac{\mathrm{Im}[\{f(X_i + i\Delta X_i)\}]}{\Delta X_i} - \frac{\mathrm{Im}[[K(X_i + i\Delta X_i)]]}{\Delta X_i}\{u\}\right\} \tag{25}$$

The computation of $\mathrm{Im}[f(X + i\Delta X)]/\Delta X$ and $\mathrm{Im}[K(X + i\Delta X)]/\Delta X$ vectors can be performed in an element-by-element fashion so as to avoid the creation of a global complex vector or matrix. This reduces memory requirements by a factor of two and processing time requirements by a factor of three or more. The factored stiffness matrix used for computing the displacements is reused for computing each of the sensitivities. With this approach, a large number of design variables can be handled efficiently as each requires only a single back solve.
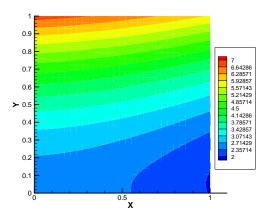
Fig. 9. Case 1: Distribution of *E(x,y)* used for the forward solution

Fig. 10. Case 1: Distribution for E(x,y) inversely determined using measured internal displacements
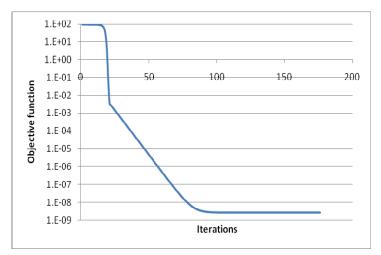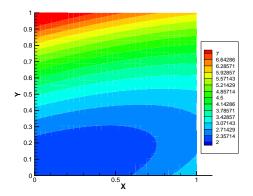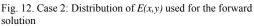

Fig. 11. Convergence history for Case 2

3.3 Numerical Results

In this section, the inverse formulation given in section 3.1 will be demonstrated using two cases. In the first case, measurements of deflection at four locations in the plate are used to inversely determine the spatial variation of elasticity modulus coefficients, *{E}*. In the second case, the reaction force and moment are used at four locations as the measurements. In both cases, simulated measurements were used that were obtained from the forward solution without additional measurement errors. The analysis model used for both cases was described in section 3.1 and was shown in Fig. 7. The forward problem was created by setting *{E}={2.0 MPa, 3.0 MPa, 6.0 MPa, 8.0 MPa}*. For both cases a gradient-based unconstrained non-linear optimization algorithm (Optimization Toolbox, 2008) was used to minimize the objective function, Equation 19. The objective function value and the gradients were computed using CVSAM finite element program.

For the first case, the sensitivities of the displacement, *w*, with respect to the design variables {E} were computed for the forward problem. The four nodes with the largest sensitivities were selected as simulated measurement points. The displacements at these points were then used to formulate the objective function given by Equation (19). An initial guess of *{E} = {5.0 MPa, 5.0 MPa, 5.0 MPa, 5.0 MPa}* was used. The convergence history for this case is shown in Fig. 8. The optimized design variables were *{E} = {2.52 MPa, 1.98 MPa, 5.88 MPa, 6.84 MPa}*. A graphical comparison between the exact and inverse solution is shown in Figures 9 and 10. The maximum error in the predicted value of *E(x,y)* was 30% and is located at the lower right corner of the plate. These results show that this problem is very ill-conditioned in that even the slightest error in the measurements results in a much larger error in the predicted modulus.
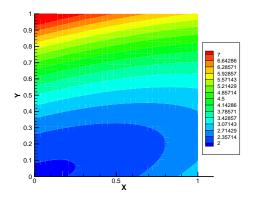
Fig. 12. Case 2: Distribution of *E(x,y)* used for the forward solution

Fig. 13. Case 2: Predicted *E(x,y)* using measured F_z and *M* on the boundaries

In the second case, measurements of reaction forces and moments on the fixed boundaries were used. The reaction force, F_z, and the reaction bending moment, *M,* at four boundary points were taken from the forward solution as simulated measurements. The initial guess for the values of the modulus of elasticity was the same as used in case 1. The convergence history is shown in Fig. 11. By iteration 100, the objective function was less than 3.0e-9. The design variables for the minimum value were *E={1.96 MPa,2.94 MPa,5.88 MPa,7.84 MPa}*. A graphical comparison between the exact and inverse solution is shown in Figures 12-13. The maximum error in the predicted *E(x,y)* is 2.0%, an order of magnitude lower than in case 1.

The results demonstrate that for this case using measurements of reaction forces and moments lead to more accurate estimation of *E(x,y)* than measurements based on displacement. However, both approaches exhibit significant amplification of measurement error that is typical of ill-conditioned problems. For practical applications, this method would require regularization as physical measurements are likely to have errors greater than 1%.

3.4 Conclusions Concerning Approaches to Inverse Determination of Elasticity Modulus

An inverse approach was presented, that is based on non-linear optimization, to inversely determine anisotropic modulus of elasticity in a transversely loaded plate. The sensitivities used for the optimization were computed accurately and efficiently for the finite element model using the complex variable semi-analytic method. Two cases were examined; one was based on simulated measurements of displacements and the other based on simulated measurements of boundary forces and moments. The latter approach predicted the modulus of elasticity with a maximum error of 2.0% using simulated measurements at four points. While both cases exhibit signs of ill-conditioning, the errors could potentially be further reduced by introducing regularization.

4 Summary

Applications of the finite element method to iterative solution of inverse problems of finding unknown boundary conditions and to inverse problem of finding spatial variation of the modulus of elasticity were presented and demonstrated. Both formulations involved the use of simulated boundary measurements to inversely predict desired quantities that were spatially varying. While the examples shown here were successful, more work is required to extend these approaches to large scale multiply connected three-dimensional non-isotropic objects with realistic measurement errors of accessible boundary conditions.

References

Barthelemy, B., Chon, C. T. and Haftka, R. T., 1988, "Accuracy Problems Associated with Semi-Analytical Derivatives of Static Response," *Finite Elements in Analysis and Design*, **4**, pp. 249-265.

Barthelemy, B. and Haftka, R. T., 1990, "Accuracy Analysis of the Semi-Analytical Method for Shape Sensitivity Calculation," *Mech. Struc. & Mach.*, **18**, no 3, pp. 407-432.

Cheng, G., Gu, Y. and Zhou, Y., 1989, "Accuracy of Semi-analytical Sensitivity Analysis," *Finite Elements in Analysis and Design*, **6**, pp. 113-128.

Comino, L. and Gallego, R., 2005, "Material Constants Identification in Anisotropic Materials Using Boundary Element Techniques," *Inverse Problems in Science and Engineering*, **13**, pp 635 – 654.

Cooreman, S., Lecompte, D., Sol, H., Vantomme, J. and Debruyne, D., 2007, "Elasto-plastic Material Parameter Identification by Inverse Methods: Calculation of the Sensitivity Matrix," *International Journal of Solids and Structures*, **44,** pp. 4329-4341.

Dennis, B. H. and Dulikravich, G. S., 1999, "Simultaneous Determination of Temperatures, Heat Fluxes, Deformations, and Tractions on Inaccessible Boundaries," *ASME Journal of Heat Transfer*, **121**, pp. 537–545.

Dennis, B. H., Dulikravich, G. S. and Yoshimura, S., Feb. 2004, "A Finite Element Formulation for the Determination of Unknown Boundary Conditions for 3-D Steady Thermoelastic Problems," *ASME Journal of Heat Transfer*, **126**, pp. 110–118.

Furukawa , T., Michopoulos, J. G. and Kelly, D. W., 2008, "Elastic Characterization of Laminated Composites Based on Multiaxial Tests," *Composite Structures*, **86**, pp. 269–278.

Hensel, E. H. and Hills, R., 1989, "Steady-State Two-Dimensional Inverse Heat Conduction," *Numerical Heat Transfer*, **15**, pp. 227–240.

Huebner, K. H., Thorton, E. A. and Byrom, T. G., 1995, *The Finite Element Method for Engineers*. John Wiley and Sons, New York, NY, third edition.

Hughes, T. J. R., 2000, *The Finite Element Method: Linear Static and Dynamic Finite Element Analysis*. Dover Publications, Inc., New York.

Jin, W., Dennis, B. H. and Wang, B. P., 2009, "Improved Sensitivity and Reliability Analysis of Nonlinear Euler-Bernoulli Beam Using a Complex Variable Semi-Analytical Method," Proceedings of the ASME International Design Engineering Technical Conferences & Computers and Information in Engineering Conference (IDETC/CIE 2009), No. DETC2009-87593, Aug. 30 – Sept. 2, San Diego, CA.

Jin, W., Dennis, B. H. and Wang, B. P., 2010a, "Improved Sensitivity Analysis Using a Complex Variable Semi-analytical Method," *Struc. Multidisciplinary Optim.*, **41**, no 3, pp. 433-439.

Jin, W., Dennis, B. H. and Wang, B. P., 2010b, "Sensitivies Analysis Using the Semi-Analytic Complex Variable Method in Fracture Mechanics," Proceedings of the ASME International Design Engineering Technical Conferences & Computers and Information in Engineering Conference (IDETC/CIE 2010), No. DETC2010-29130, Aug. 15-18, Montreal, Quebec, Canada.

Larsen, M. E., 1985, "An Inverse Problem: Heat Flux and Temperature Prediction for a High Heat Flux Experiment," Tech. rep. SAND-85-2671, Sandia National Laboratories, Albuquerque, NM.

Lee, T. H., 1999, "An Adjoint Variable Method for Design Sensitivity Analysis of Elastoplastic Structures", *J. Mechanical Science & Technology*, **13**, pp. 246-252.

Liu, P. L. and Der Kiureghian, A., 1989, "Finite Element Reliability Methods for Geometrically Non Linear Stochastic Structures," Tech. Rep. No. UCB/SEMM/89-05, University of California, Berkeley, CA.

Martin, T. J., Halderman, J. and Dulikravich, G. S., 1995, "An Inverse Method for Finding Unknown Surface Tractions and Deformations in Elastostatics," *Computers and Structures*, **56**, pp. 825–836.

Martin, T. J. and Dulikravich, G. S., 1996, "Inverse Determination of Boundary Conditions in Steady Heat Conduction," *ASME Journal of Heat Transfer*, **3**, pp. 546–554.

Martins, J. R .R. A., Sturdza P. and Alonso, J. J., 2003, "The Complex-Step Derivative Approximation," *ACM Transactions on Mathematical Software*, **29**, 3, pp. 245-262.

Neumaier, A., 1998, "Solving Ill-Conditioned and Singular Linear Systems: A Tutorial on Regularization," *SIAM Review*, **40**, pp. 636–666.

Olhoff, N. and Rasmussen, J., 1991, "Study of Inaccuracy in Semi-analytical Sensitivity Analysis - A Model Problem," *Structural Optimization*, **3**, pp. 203-213.

Olson, L. G. and Throne, R. D., 2000, "The Steady Inverse Heat Conduction Problem: A Comparison for Methods of Inverse Parameter Selection," in *34th National Heat Transfer Conference-NHTC'00*, No. NHTC2000-12022, Pittsburg, PA.

Optimization Toolbox, Matlab Documentation, 2008.

Paige, C. C. and Saunders, M. A., 1982, "LSQR: An Algorithm for Sparse Linear Equations and Sparse Least Squares," *ACM Transactions on Mathematical Software*, **8**, pp.43 -71.

Yuan, F.G. and Özisik, M. N., 1996, "Determination of elastic constants by inverse analysis," *Inverse Problems in Science and Engineering*, **3**, pp. 1–19.

Zhang, S.-U. and Kumar, A. V., 2010, "Damage Sensing by Inverse Estimation of Electrical Resistivity of Composite Structure," Proceedings of the ASME International Design Engineering Technical Conferences & Computers and Information in Engineering Conference (IDETC/CIE 2010), Aug 15-18, Montreal, Quebec, Canada.

Zhang, Y. and Der Kiureghian, A., 1993, "Dynamic Response Sensitivity of Inelastic Structures," *Comp. Meth. Appl. Mech. Eng.*, **108**, pp. 23-26.